

# Adaptive Modulation in Ad Hoc DS/CDMA Packet Radio Networks

Michael R. Souryal, *Member, IEEE*, Branimir R. Vojcic, *Senior Member, IEEE*, and Raymond L. Pickholtz, *Life Fellow, IEEE*

**Abstract**—This paper investigates the benefit of adaptive modulation based on channel state information (CSI) in direct-sequence/code-division multiple-access (DS/CDMA) multihop packet radio networks. By exploiting varying channel conditions, adaptive modulation can be used in ad hoc networks to provide upper layers with higher capacity links over which to relay traffic. Using the  $\alpha$ -stable interference model, the distribution of the signal-to-interference ratio (SIR) is obtained for a slotted system of randomly, uniformly distributed nodes using multilevel coherent modulation schemes. Performance is evaluated in terms of the information efficiency, which is a new progress-related measure for multihop networks. Three types of adaptivity are analyzed, differing in the level of CSI available: 1) full knowledge of the SIR at the receiver; 2) knowledge of only the signal attenuation due to fading; and 3) knowledge of only the slow fading component of the signal attenuation. The effect of imperfect channel information is also investigated. Sample results are given for interference-limited networks experiencing fourth-power path loss with distance, Rician fading, and lognormal shadowing.

**Index Terms**—Adaptive modulation, cochannel interference, code-division multiaccess, packet radio.

## I. INTRODUCTION

AD HOC packet radio networks are collections of self-organized autonomous radio terminals that communicate peer to peer over a dynamic, infrastructure-less topology. Their decentralized structure favors the use of the shared radio channel by random access, which, combined with mobility and multipath fading, can lead to highly dynamic channel quality. Adaptive transmission has long been considered as a means to improve communication performance in dynamic channels. This paper investigates the use of adaptive modulation at the physical layer to increase the efficiency of ad hoc direct-sequence/code-division multiple-access (DS/CDMA) networks. In ad hoc networks, multihop relaying permits

communication between nodes that are not in range of one another [1]. Therefore, the measure of performance used in this analysis, and which governs the adaptive modulation function, accounts for not only the throughput of the link but also the progress it offers to the packet's ultimate destination.

Because of the effects of fading and/or shadowing, which are modeled as random variations in the path loss, some links are able to reliably carry more information than others, even among links of comparable distance. Furthermore, in mobile networks, the capacity of a given link can change over time. Using knowledge of the instantaneous channel state, adaptive transmission exploits this variability to improve link efficiency [2]–[4]. For example, with adaptive modulation, a larger constellation is used on links with favorable channel conditions, and, conversely, a more robust scheme is used on poorer links. Alternatively, if the objective is to conserve energy, channel state information (CSI) could be used to adjust the transmission power to the minimum level required for a given quality of service. In [2], both modulation and power were adapted to maximize spectral efficiency. When power was kept constant and the modulation varied, the loss compared to the discrete rate-continuous power scheme was only 1–2 dB for an uncoded system. An analysis of adaptive modulation in cellular systems found similarly that most of the gain in throughput of a combined adaptive modulation and power scheme could be achieved with a much simpler adaptive modulation-fixed power scheme [3].

Much of the previous work on adaptive modulation addresses two-user or cellular systems. This paper considers the use of adaptive modulation in the context of ad hoc multihop packet radio networks. A key differentiating characteristic in these networks is the nature of the multiple-access interference (MAI), which can change rapidly over time. Of interest is not only the overall potential gain of adaptive modulation, but also the gain when the adaptation is performed with respect to the more slowly varying channel attenuation, without knowledge of the instantaneous interference.

An integral element of this analysis, therefore, is the characterization of the MAI, for which previous work has provided useful models. In [5], the distribution of the interference power was derived for slotted DS/CDMA networks of randomly, uniformly distributed nodes on a plane (or, equivalently, nodes distributed according to a Poisson process in two dimensions). In [6], the distribution of the interference in a Poisson field of interferers was shown to be  $\alpha$ -stable, and the result was applied to the analysis of both DS and frequency-hopping networks for the case of deterministic ground-wave propagation. An alternative proof of the  $\alpha$ -stable interference result was given in

Paper approved by G. E. Corazza, the Editor for Spread Spectrum of the IEEE Communications Society. Manuscript received September 19, 2003; revised June 4, 2005 and October 31, 2005. This work was supported in part by the National Science Foundation under Grant CCF-0429228. This paper was presented in part at the IEEE Military Communications Conference (MILCOM), Boston, MA, October 2003, and in part at the IEEE Global Communications Conference (GLOBECOM), San Francisco, CA, December 2003.

M. R. Souryal was with the Department of Electrical and Computer Engineering, The George Washington University, Washington, DC 20052 USA. He is now with the Wireless Communication Technologies Group, National Institute of Standards and Technology, Gaithersburg, MD 20899-8920 USA (e-mail: souryal@nist.gov).

B. R. Vojcic and R. L. Pickholtz are with the The George Washington University, Washington, DC 20052 USA (e-mail: vojic@gwu.edu; pickholt@gwu.edu).

Digital Object Identifier 10.1109/TCOMM.2006.873092

[7], where the model also incorporated stochastic propagation models and where the performance of various detectors was evaluated. These models are extended to account for networks in which multiple two-dimensional (2-D) constellations are used.

A second characteristic that differentiates this study from previous work on adaptive modulation is the use of a progress-related performance measure that is of particular relevance to multihop networks. In [5], [8], and [9], the expected progress per hop was the performance measure with respect to which network parameters such as transmission range were optimized. This measure is a function of the local one-hop throughput and the progress made by a hop toward the final destination, both of which impact end-to-end throughput. In [10] and [11], a spectral efficiency factor was incorporated into the expected progress, and the new measure (information efficiency) was used to evaluate the performance of different code rates. However, none of this work addressed adaptive techniques. Here, we evaluate the benefit of adaptive modulation in terms of information efficiency and use it to identify the optimum tradeoff between short, high-capacity hops and long, high-progress hops in an adaptive system.

The analysis applies to DS/CDMA networks in which the objective is to maximize system throughput for a given level of expended energy per transmission.<sup>1</sup> Since adaptive modulation depends on knowledge of the channel state, three varieties of adaptivity are considered, depending on the level of knowledge available: knowledge of: 1) both the signal attenuation and interference; 2) of the signal attenuation only; and 3) of only the slow fading component of the signal attenuation. The impact on performance of imperfect channel information is considered, as well.

The remainder of the paper is organized as follows. Section II describes the system model for the analysis and the performance measure. In Section III, the  $\alpha$ -stable interference model is applied to systems using multilevel coherent modulation schemes. A performance analysis of the adaptive systems is given in Section IV for interference-limited networks. Lastly, Section V summarizes the key conclusions.

## II. SYSTEM MODEL AND PERFORMANCE MEASURE

As in [5], a system of packet radio network terminals is modeled as a Poisson field of interferers (i.e., randomly, uniformly distributed in the plane) with an average density of  $\lambda$  nodes per unit area. The system is slotted, and a node transmits a frame with probability  $p$  in any given slot. Transmissions are made using DS/CDMA, which is modeled with random spreading and asynchronism at the chip level. The transmitted energy per symbol is assumed to be fixed and the same for all nodes. Furthermore, the traffic matrix is uniform.

A node's transmission uses one of several coherent modulation schemes that differ in spectral efficiency and robustness to interference. A given modulation scheme is used for the entire frame, and the scheme can be changed from frame to

<sup>1</sup>While energy conservation is not the primary objective here, there are some energy savings associated with increased throughput when the total amount of information to be transmitted is fixed. The savings come as a result of reducing the number of (fixed-length) packet transmissions through higher spectral efficiency signaling.

frame depending on link conditions. In practice, the preamble of the frame can be encoded using the lowest order modulation scheme, and a field in the preamble can indicate which modulation scheme is used for the payload, as in IEEE 802.11b [12].

The distance between any two nodes is assumed to be greater than the far-field distance of the antenna. The overall channel attenuation on a link is a combination of large-scale path loss, with path-loss exponent  $m$ , and a random attenuation  $\mathcal{C}$  due to frequency-flat fading and/or shadowing. As a result, the power received from a node transmitting with power  $P_T$  at a distance  $r$  from the receiver is proportional to  $\mathcal{C}P_T/r^m$ . The fading/shadowing attenuation  $\mathcal{C}$  is normalized to have unit mean. Furthermore, it is assumed to be sufficiently slow that it is approximately constant during a time slot.

Strong forward error correction (FEC) based on parallel concatenated convolutional codes (PCCCs) and iterative decoding, or "turbo" codes, is assumed, for which the probability of error is a steep function of the signal-to-noise ratio (SNR). Therefore, the probability of successful transmission of a frame is modeled as the probability that the SNR during the slot exceeds a threshold

$$P_s = \Pr[\text{SNR} > \mu_c] = 1 - F_\mu(\mu_c) \quad (1)$$

where  $F_\mu(\cdot)$  is the cumulative distribution function of the SNR and  $\mu_c$  is the threshold, or cut-off SNR.<sup>2</sup> The cut-off value, in turn, is a function of the modulation-coding scheme.

In a multihop ad hoc network in which messages are retransmitted by relays on route to the destination, overall throughput is impacted not only by the throughput of each link, but also by the distance, or progress, the message makes toward its final destination on each hop. A greater progress per hop results in fewer hops (meaning fewer retransmissions) as well as fewer nodes being occupied by relaying, thereby allowing them to transmit or receive their own traffic. Furthermore, for a given transmission energy, link distance and link throughput tend to be inversely related, which is a key tradeoff in relay selection. Maximizing system throughput, then, involves optimizing this tradeoff between the number of hops a message must take and the message throughput per hop. One performance measure that captures this tradeoff is the *information efficiency*, which is defined as the product of the progress (in distance) made by the transmission toward the final destination and the local throughput on the link, where the throughput incorporates the spectral efficiency of the modulation-coding scheme [10], [11]. For the described system, the information efficiency, when normalized by the square root of the node density, is [11]

$$IE = \sqrt{\frac{N}{\pi}} \tau(p) \epsilon P_s \quad (2)$$

where  $\tau(p) = (1-p)(1-e^{-p})$  is the probability that two nodes pair up [5],  $\epsilon$  is the spectral efficiency in b/s/Hz of the

<sup>2</sup>Frames with errors not corrected by FEC are typically recovered at a higher layer through retransmission (e.g., using automatic repeat request (ARQ) at the link layer).

modulation-coding scheme, and  $N$  is a dimensionless measure of hop distance defined as the average number of nodes in a disc of radius  $R$

$$N \triangleq \lambda\pi R^2. \quad (3)$$

(For a link distance of  $R$ ,  $N$  can be interpreted as the average number of nodes that are closer to the receiver than the transmitter. It is a measure of the average number of nodes being ‘‘hopped over.’’) When multiplied by the channel bandwidth and divided by the square root of the node density ( $\sqrt{\lambda}$ ), the de-normalized information efficiency has units of b·m/s, alternately referred to as the speed with which a bit travels through the network [10] or the per-user transport capacity [13].

### III. INTERFERENCE MODEL

#### A. Detector Output

For the described system, the received signal at a node during a symbol period  $0 < t < T_s$  is

$$r(t) = \sum_k \sqrt{\frac{C_k E_T}{2r_k^m}} [a_{I,k} s_{I,k}(t; \theta_k, \tau_k) + a_{Q,k} s_{Q,k}(t; \theta_k, \tau_k)] + n(t) \quad (4)$$

where the summation is over all transmitting nodes;  $C_k$  and  $r_k$  are the fading attenuation and distance of node  $k$  from the receiver, respectively,  $E_T$  is proportional to the transmitted symbol energy,  $a_{I,k}$  and  $a_{Q,k}$  are the in-phase and quadrature information-bearing amplitudes of node  $k$  (each with unit mean square value), and  $n(t)$  is a white Gaussian noise process with two-sided power spectral density  $N_0/2$ . Signals  $s_{I,k}(t; \theta_k, \tau_k)$  and  $s_{Q,k}(t; \theta_k, \tau_k)$  are unit energy-spreading waveforms defined as

$$\begin{aligned} s_{I,k}(t; \theta_k, \tau_k) &= \sqrt{\frac{2}{T_s}} \cos(\omega_c t + \theta_k) \\ &\quad \times \sum_{n=0}^{G-1} c_{I,k,n} h(t - \tau_k - nT_c) \\ s_{Q,k}(t; \theta_k, \tau_k) &= \sqrt{\frac{2}{T_s}} \sin(\omega_c t + \theta_k) \\ &\quad \times \sum_{n=0}^{G-1} c_{Q,k,n} h(t - \tau_k - nT_c) \end{aligned}$$

where  $\omega_c$  is the carrier angular frequency,  $\theta_k$  and  $\tau_k$  are the phase and delay, respectively, of node  $k$ 's signals, relative to the receiver,  $\{c_{I,k,n}\}$  and  $\{c_{Q,k,n}\}$  are node  $k$ 's in-phase and quadrature (random) spreading sequences, respectively, and are assumed to be made up of independent, equiprobable  $\{+1, -1\}$  chips,  $T_c$  is the chip duration,  $G = T_s/T_c$  is the processing gain, and  $h(t)$  is a pulse of duration  $T_c$  seconds and energy  $T_c$  Joules.

Let the 2-D vector  $\mathbf{U}$  represent the outputs of the in-phase and quadrature detectors matched to the  $j$ th signal, sampled at time  $t = T_s$ , and given as

$$\begin{aligned} \mathbf{U} &= \int_0^{T_s} r(t) \mathbf{s}_j(t) dt \\ &= \sqrt{\frac{C_j E_T}{2r_j^m}} \mathbf{a}_j + \sqrt{\frac{E_T}{2}} \mathbf{Y} + \mathbf{N} \end{aligned} \quad (5)$$

where  $\mathbf{s}_j(t) = [s_{I,j}(t; \theta_j, \tau_j) \ s_{Q,j}(t; \theta_j, \tau_j)]^T$  and  $\mathbf{a}_j = [a_{I,j} \ a_{Q,j}]^T$ . The first term in (5) represents the desired signal component,  $\mathbf{N}$  is a zero-mean bivariate Gaussian random vector with covariance matrix  $(N_0/2)\mathbf{I}$  representing the contribution due to thermal noise, and the contribution due to MAI is

$$\mathbf{Y} = \sum_{k \neq j} \frac{1}{r_k^{\frac{m}{2}}} \mathbf{X}_k$$

where

$$\mathbf{X}_k = \sqrt{C_k} \mathbf{R}(\Delta_{jk}, \theta_{jk}) \mathbf{a}_k \quad (6)$$

is the contribution due to interferer  $k$ . The  $2 \times 2$  matrix  $\mathbf{R}(\Delta_{jk}, \theta_{jk})$  in (6) is the cross-correlation matrix of the  $j$ th and  $k$ th spreading waveforms, defined as

$$\mathbf{R}(\Delta_{jk}, \theta_{jk}) \triangleq \int_0^{T_s} \mathbf{s}_j(t) \mathbf{s}_k^T(t) dt$$

where  $\Delta_{jk} = |\tau_j - \tau_k|/T_c$  is the normalized relative delay between the signals of nodes  $j$  and  $k$ , and  $\theta_{jk} = \theta_j - \theta_k$  is the corresponding phase difference. The quantities  $\Delta_{jk}$  and  $\theta_{jk}$  are modeled as uniform random variables on the intervals  $(0,1)$  and  $(0, 2\pi)$ , respectively. The upper-right element of  $\mathbf{R}(\Delta_{jk}, \theta_{jk})$ , for example, can be expressed as

$$\begin{aligned} R_{IQ}(\Delta_{jk}, \theta_{jk}) &= \int_0^{T_s} s_{I,j}(t; \theta_j, \tau_j) s_{Q,k}(t; \theta_k, \tau_k) dt \\ &= \sin \theta_{jk} [H_0(\Delta_{jk}) \rho_{IQ}(j, k; 0) \\ &\quad + H_1(\Delta_{jk}) \rho_{IQ}(j, k; 1)] \end{aligned}$$

where

$$\begin{aligned} \rho_{IQ}(j, k; l) &= \frac{1}{G} \sum_{n=0}^{G-1} c_{I,j,n} c_{Q,k,n+l} \\ H_0(\Delta) &= \int_{\Delta}^1 h(\lambda T_c) h[(\lambda - \Delta) T_c] d\lambda \\ H_1(\Delta) &= \int_0^{\Delta} h(\lambda T_c) h[(\lambda - \Delta + 1) T_c] d\lambda \end{aligned} \quad (7)$$

are the cross-correlation of nodes  $j$  and  $k$ 's in-phase and quadrature spreading sequences and the partial cross-correlations of the chip pulse, respectively. For rectangular chips,  $H_1(\Delta) = \Delta = 1 - H_0(\Delta)$ .

### B. Interference Distribution

It was shown in [6] and [7] that if: 1) the interferers are distributed in an infinite plane according to a 2-D Poisson point process with parameter  $\lambda_t$  (the average number of interferers per unit area) and 2) the  $\mathbf{X}_k$  are independent and identically distributed (i.i.d.) and have a spherically symmetric probability density function, then the total interference at the detector  $\mathbf{Y}$  has a spherically symmetric  $\alpha$ -stable distribution with a characteristic function expressed as

$$\phi_{\mathbf{Y}}(\boldsymbol{\omega}) = \exp(-\sigma_Y \|\boldsymbol{\omega}\|^\alpha). \quad (8)$$

The index of stability  $\alpha$  and the dispersion parameter  $\sigma_Y$  are given by

$$\alpha = \frac{4}{m}, \quad m > 2, \quad (9)$$

$$\sigma_Y = -\pi \lambda_t \int_0^\infty \frac{\Phi'_0(x)}{x^\alpha} dx \quad (10)$$

where  $\Phi_0(\|\boldsymbol{\omega}\|) = \Phi_{\mathbf{X}}(\boldsymbol{\omega})$  is the spherically symmetric characteristic function of  $\mathbf{X}$ . (The subscript  $k$  is heretofore dropped for the i.i.d.  $\mathbf{X}_k$ .) An equivalent expression for  $\sigma_Y$  is [7]

$$\sigma_Y = \pi \lambda_t C_\alpha^{-1} \mathbb{E}[|X|^\alpha] \quad (11)$$

where

$$C_\alpha = \begin{cases} \frac{1-\alpha}{\Gamma(2-\alpha) \cos(\frac{\pi\alpha}{2})}, & \alpha \neq 1 \\ \frac{2}{\pi}, & \alpha = 1. \end{cases}$$

$X$  represents one component of the spherically symmetric random vector  $\mathbf{X}$ , and  $\Gamma(\cdot)$  is the gamma function.

The first condition for (8) is met by definition of the system model, with  $\lambda_t = \lambda p$ . Using an analysis similar to that given in [6], it can be shown that, for the second condition,  $\mathbf{X}$  is nearly spherically symmetric provided the processing gain is nonnegligible [14]. In this case,  $\mathbb{E}[|X|^\alpha]$  in (11) is given by [14]

$$\mathbb{E}[|X|^\alpha] = \sqrt{\frac{2^\alpha}{\pi G^\alpha}} \Gamma\left(\frac{\alpha+1}{2}\right) \mathbb{E}[\mathcal{C}^{\frac{\alpha}{2}}] \delta_\alpha \chi_\alpha \quad (12)$$

where

$$\begin{aligned} \delta_\alpha &= \mathbb{E}\left\{[H_0^2(\Delta) + H_1^2(\Delta)]^{\frac{\alpha}{2}}\right\} \\ \chi_\alpha &= \mathbb{E}\left[(a_I^2 \cos^2 \theta + a_Q^2 \sin^2 \theta)^{\frac{\alpha}{2}}\right]. \end{aligned} \quad (13)$$

The expectation on the right-hand side of (12) is the  $\alpha/2$ -moment of the channel gain. The factor  $\delta_\alpha$  is evaluated using the fact that  $\Delta$  is uniformly distributed on  $(0,1)$ . The factor  $\chi_\alpha$  is likewise evaluated from the uniform distribution of  $\theta$  on  $(0, 2\pi)$  as well as a probability assignment on the modulation schemes in use.

In evaluating the success probability (1), we require the energy of the interference during a slot. Now, for any  $\alpha$  in the range allowed by (9) ( $0 < \alpha < 2$ ), the second moment of a stable random variable does not exist. However, using the fact that a symmetric stable random vector is sub-Gaussian with an underlying Gaussian vector having i.i.d. zero-mean Gaussian components, the  $\alpha$ -stable random vector  $\mathbf{Y}$  can be expressed as the product

$$\mathbf{Y} = \sqrt{V} \cdot \mathbf{G}$$

where  $\mathbf{G}$  is a zero-mean Gaussian vector with identity covariance matrix and  $V$  is an  $\alpha/2$ -stable random variable totally skewed to the right and independent of  $\mathbf{G}$  [15]. The scale parameter of  $V$  in terms of  $\sigma_Y$  is

$$\sigma_V = 2 \left[ \sigma_Y \cos\left(\frac{\pi\alpha}{4}\right) \right]^{\frac{2}{\alpha}}.$$

The interpretation of this result for a DS/CDMA system with random spreading is that, in a given time slot, the MAI is, for large processing gain, modeled as conditionally Gaussian, conditioned on the distances of the interferers from the receiver, their relative phases and chip delays, and their fading attenuations during that slot. Once the conditioning is removed (i.e., the randomness of these quantities from slot to slot is taken into account), the distribution of the MAI is no longer Gaussian but is  $\alpha$ -stable,  $0 < \alpha < 2$ . The MAI can be viewed, however, as Gaussian with the random variance, or interference energy  $V$ , accounting for the randomness of the distances, phases, and chip delays of the interferers. This analysis of the MAI as conditionally Gaussian with random variance is another form of the ‘‘improved Gaussian approximation’’ [16].

The density and distribution functions of the  $\alpha/2$ -stable random variable  $V$  can be expressed as convergent series [17, pp. 89–90], [18, pp. 581–583]. For  $0 < \alpha < 2$ , they are

$$\begin{aligned} f_V(v) &= \frac{1}{\pi v} \sum_{n=1}^{\infty} (-1)^{n-1} \frac{\Gamma(n\alpha' + 1)}{n!} \sin(n\pi\alpha') \left(\frac{\rho}{v}\right)^{n\alpha'} \\ F_V(v) &= 1 - \frac{1}{\pi} \sum_{n=1}^{\infty} (-1)^{n-1} \frac{\Gamma(n\alpha')}{n!} \sin(n\pi\alpha') \left(\frac{\rho}{v}\right)^{n\alpha'} \end{aligned} \quad (14)$$

for  $v > 0$ , where  $\alpha' = \alpha/2$  and

$$\rho = \sigma_V \cos^{-\frac{1}{\alpha'}} \left( \frac{\pi\alpha'}{2} \right) = 2\sigma_Y^{\frac{2}{\alpha}}.$$

In the case of a fourth-power path loss with distance ( $m = 4$ ), the distribution of the interference energy  $V$  can be simplified.

In this case,  $\alpha = 1$  and  $V$  is 1/2-stable with parameter  $\sigma_V = \sigma_Y^2$ , corresponding to the Lévy distribution with density and distribution functions

$$\begin{aligned} f_V(v) &= \frac{\sigma_Y}{\sqrt{2\pi}} v^{-\frac{3}{2}} \exp\left(-\frac{\sigma_Y^2}{2v}\right), \quad v > 0 \\ F_V(v) &= \operatorname{erfc}\left(\frac{\sigma_Y}{\sqrt{2v}}\right), \quad v > 0. \end{aligned} \quad (15)$$

### C. Frequency-Selective Fading

Although the preceding analysis assumed frequency-flat fading, we show in this section how frequency-selective fading can be incorporated into the interference model and that its effect is simply to scale the dispersion parameter.

Modeling the frequency-selective channel from an interferer as having  $L$  distinct components with gains  $C_{kl}$ , phase shifts  $\theta_{kl}$ , and delays  $\tau_{kl}$ ,  $l = 1, \dots, L$ , then the received signal (4) becomes

$$\begin{aligned} r(t) &= \sum_k \sqrt{\frac{E_T}{2r_k^m}} \sum_{l=1}^L \sqrt{C_{kl}} [a_{I,k} s_{I,k}(t; \theta_{kl}, \tau_{kl}) \\ &\quad + a_{Q,k} s_{Q,k}(t; \theta_{kl}, \tau_{kl})] + n(t). \end{aligned}$$

The contribution due to interferer  $k$  [see (6)], in turn, becomes a sum

$$\mathbf{X}_k = \sum_{l=1}^L \sqrt{C_{kl}} \mathbf{R}(\Delta_{jkl}, \theta_{jkl}) \mathbf{a}_k$$

where now  $\Delta_{jkl} = |\tau_j - \tau_{kl}|/T_c$  and  $\theta_{jkl} = \theta_j - \theta_{kl}$ .

Following the approach used to obtain (12) and dropping the subscripts  $j$  and  $k$ , the absolute  $\alpha$ -moment of each component of  $\mathbf{X}$  in the case of frequency-selective fading is

$$\begin{aligned} \mathbb{E}[|X|^\alpha] &= \sqrt{\frac{2^\alpha}{\pi G^\alpha}} \Gamma\left(\frac{\alpha+1}{2}\right) \\ &\quad \times \mathbb{E}\left[\left\{\sum_{l=1}^L C_l [H_0^2(\Delta_l) + H_1^2(\Delta_l)] \right. \right. \\ &\quad \left. \left. \times (a_I^2 \cos^2 \theta_l + a_Q^2 \sin^2 \theta_l) \right\}^{\frac{\alpha}{2}}\right] \end{aligned} \quad (16)$$

which, with (11), gives the dispersion parameter of the interference. Note that (12) and (16) are equivalent for  $L = 1$ .

We observe, then, that the effect of frequency selectivity on the interference is simply a scaling of its dispersion. Furthermore, no assumption was made as to the correlation of the multipath components, so the above result applies both to correlated as well as uncorrelated scattering. In general, it is the Poisson distribution of the interferer positions that leads to the  $\alpha$ -stable distribution of the interference and the statistics of the interferer signal and channel that scale its dispersion.

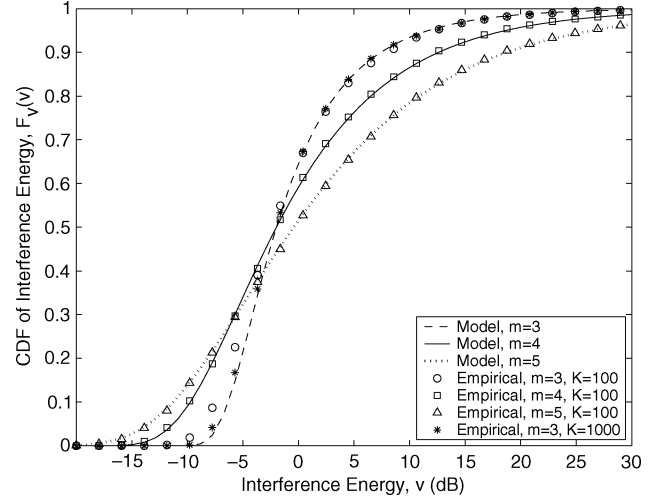


Fig. 1. Cumulative distribution function of the interference energy: comparison of analytical and empirical results for different path-loss exponents  $m$  and number of interferers  $K$ .

### D. Comparison With Simulation Results

The analytical result for the distribution of the interference energy is compared with simulation results at the center of a network of  $K$  uniformly distributed interferers, where each interferer signal uses quaternary phase-shift keying (QPSK), 16-quadrature-amplitude modulation (16-QAM), or 64-QAM modulation with probability assignment  $\{0.5, 0.4, 0.1\}$ , respectively, rectangular chips, and processing gain  $G = 11$ . The channel is characterized by flat Rayleigh fading and 8-dB lognormal shadowing. Fig. 1 illustrates the analytical model and empirical results for three different path-loss exponents. The model is observed to be quite accurate for  $m = 4$  and  $m = 5$ , while for  $m = 3$  the simulated results deviate from the predicted somewhat for a network size of  $K = 100$  interferers. The actual number of interferers in the simulated system impacts the convergence of the predicted and simulated results. Because the model is based on an idealized infinite network, the simulated results converge to the model's predicted result as the number of interferers in the system increases. The convergence is slower when the path-loss exponent is smaller, since the impact of nodes further away is greater. Increasing the simulated network size to  $K = 1000$  interferers, for example, narrows the gap between the model and empirical results for  $m = 3$ , as shown in the figure.

The system model assumes that transmissions are slot-synchronous, implying that interference energy is fixed for the duration of a slot. While slot synchronism can be achieved among a group of nodes in proximity to one another through distributed beaconing (as in an IEEE 802.11 ad hoc network, for example), it is not reasonable to assume that all nodes in a large network will be slot-synchronous, absent an external clock source such as GPS. Therefore, some interferers' transmissions will start or end during the desired signal transmission, which is not accounted for in the preceding analysis. We observe, though, that the distribution of the interference is dominated by the transmissions of the nearest interferers, which are

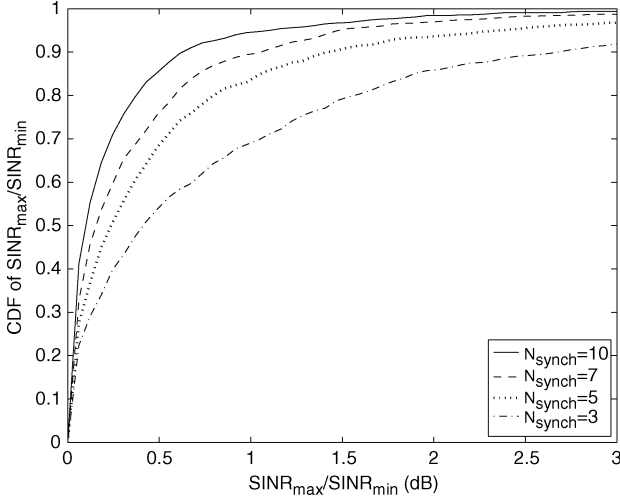


Fig. 2. Empirical cumulative distribution function of the ratio of the maximum SINR to minimum SINR during a transmission, for different radii of synchronous interferers, path-loss exponent  $m = 4$ , and 100 total interferers.

precisely the transmissions that would be slot-synchronous with the desired transmission. Though farther interferers are slot-asynchronous, their impact on the received signal-to-interference-and-noise ratio (SINR) is diminished. Fig. 2 illustrates empirical results for the cumulative distribution of the ratio of the maximum symbol SINR to minimum symbol SINR during a 1500-symbol transmission based on simulations of 100 QPSK interferers, of which the nearest  $N_{\text{synch}}$  interferers, on average, are slot-synchronous with the transmitter and the remaining interferers are asynchronous, with transmissions starting or ending at times uniformly distributed in the slot. The average SNR (in the absence of interference and fading) was set to 10 dB. For  $N_{\text{synch}} \geq 3$ , the median maximum-to-minimum ratio of SINR during a slot is less than 0.5 dB. For  $N_{\text{synch}} = 7$ , the SINR deviates by no more than 1 dB 90% of the time. Thus, it appears that the interference model can be useful even when only limited, localized slot synchronization is available.

The analysis above implicitly assumes that the channel gains  $C_k$  of the interferers' signals are independent (to satisfy the requirement that the  $\mathbf{X}_k$ 's be independent). While this is a good assumption for small-scale fading, the shadowing on two different links to the same receiver can be correlated when the angle-of-arrival difference (AAD) between them is small. In previous related work [7], [9], shadowing on different interferer links was assumed to be independent. We tested this assumption through simulation using the AAD/distance-dependent cross-correlated shadowing models proposed in [19] and found the interference model above to provide a good approximation for a mixture of independent Rayleigh fading and lightly correlated lognormal shadowing (e.g., model "1.0/0.0 R6" in [19]) or when the standard deviation (in decibels) of the shadowing is small. In general, the effect of correlation in the shadowing is to slightly shift the distribution of the interference energy to lower values. Thus, performance results based on the interference model above are slightly pessimistic for environments with cross-correlated shadowing.

#### IV. PERFORMANCE ANALYSIS

In this section, the distribution of the SINR is obtained using the result for the distribution of the interference energy in Section III. The information efficiency for a nonadaptive interference-limited system is then evaluated and compared with that of various adaptive systems.

##### A. Distribution of the SINR

For a transmitter-receiver separation  $R$ , the SINR of a channel symbol at the output of the detector is a function of the random signal gain due to fading/shadowing  $C$  and the random interference energy  $V$  as follows:

$$\mu = \frac{CE_T}{N_0 + E_T V}.$$

In terms of (14), the conditional distribution of the SINR (conditioned on  $C$ ) is

$$F_{\mu|C}(\mu'|\gamma) = \begin{cases} 1 - F_V\left(\frac{\gamma}{R^m \mu'} - \frac{N_0}{E_T}\right), & 0 < \mu' < \frac{\gamma E_T}{R^m N_0} \\ 1, & \mu' \geq \frac{\gamma E_T}{R^m N_0} \end{cases} \quad (17)$$

and the unconditional distribution of the SINR is obtained by averaging over the fading attenuation

$$F_{\mu}(\mu') = \int_0^{\infty} F_{\mu|C}(\mu'|\gamma) f_C(\gamma) d\gamma. \quad (18)$$

While the distribution of the SINR can be obtained for any path-loss exponent  $m > 2$  using (14), (17), and (18), for ease of presentation, results are given below for the special case of  $m = 4$ , which is often used to approximately model the path loss in terrestrial mobile communications.<sup>3</sup> In this case, using (15) in (17), the conditional distribution of the SINR is

$$F_{\mu|C}(\mu'|\gamma) = \begin{cases} \text{erf}\left[\frac{\sigma_Y}{\sqrt{2\left(\frac{\gamma}{R^4 \mu'} - \frac{N_0}{E_T}\right)}}\right]; & 0 < \mu' < \frac{\gamma E_T}{R^4 N_0} \\ 1; & \mu' \geq \frac{\gamma E_T}{R^4 N_0}. \end{cases}$$

For an interference-limited system (i.e.,  $N_0/E_T \rightarrow 0$ ) that is designed for maximum spectral efficiency, the conditional distribution of the SIR simplifies further to

$$F_{\mu|C}(\mu'|\gamma) = \text{erf}\left(\sigma_Y R^2 \sqrt{\frac{\mu'}{2\gamma}}\right) = \text{erf}\left(\frac{\beta N_P}{\pi} \sqrt{\frac{\mu'}{2\gamma}}\right) \quad (19)$$

for  $\mu' > 0$ , where (3) was used in the second equality and  $\beta \triangleq \sigma_Y/\lambda_t$ .

<sup>3</sup>In shadowed urban cellular radio environments, typical path-loss exponents range from 3 to 5 [20].

The distribution of the unconditional SIR can be obtained in closed form when the channel gain  $\mathcal{C}$  is due to Rayleigh fading. In this case, for unit average channel gain,  $f_{\mathcal{C}}(\gamma) = e^{-\gamma}$ . Evaluating (18) with (19) using [21, eq. (6.284)] yields

$$F_{\mu}(\mu') = 1 - \exp\left(-\frac{\beta N p}{\pi} \sqrt{2\mu'}\right) \quad (20)$$

where in the Rayleigh fading case  $E[\sqrt{\mathcal{C}}] = \sqrt{\pi}/2$  and therefore  $\beta = (\pi^2/2\sqrt{2G})\delta_1\chi_1$ .

In other cases, (18) is evaluated numerically with the appropriate density  $f_{\mathcal{C}}(\gamma)$  and mean envelope  $E[\sqrt{\mathcal{C}}]$  for  $\beta$  in (19). For example, for Ricean fading with unit average energy gain and Rice factor  $K$  (which is the ratio of specular power to scattered power), the density of the squared envelope and the mean envelope are

$$f_{\mathcal{C}}(\gamma) = (K+1) \exp[-K - (K+1)\gamma] \times I_0\left(2\sqrt{K(K+1)\gamma}\right), \quad \gamma \geq 0$$

$$E[\sqrt{\mathcal{C}}] = \frac{1}{2} \sqrt{\frac{\pi}{K+1}} e^{-K} {}_1F_1\left(\frac{3}{2}; 1; K\right)$$

where  $I_0(x)$  is the zeroth-order modified Bessel function of the first kind, and  ${}_1F_1(a, b; x)$  is the confluent hypergeometric function.

In the case of lognormal shadowing with unit average energy gain, the density and mean amplitude are

$$f_{\mathcal{C}}(\gamma) = \frac{1}{\gamma\sigma\sqrt{2\pi}} \exp\left[-\frac{1}{2\sigma^2} \left(\frac{\sigma^2}{2} + \ln \gamma\right)^2\right], \quad \gamma > 0$$

$$E[\sqrt{\mathcal{C}}] = e^{-\frac{\sigma^2}{8}}$$

where the lognormal standard deviation in decibels is  $\sigma_{\text{dB}} = 10\sigma \log_{10} e$ . Assuming that the small-scale fading and larger scale shadowing are independent, their combination can be treated by expressing the overall attenuation as the product of the two components [22]  $\mathcal{C} = \mathcal{C}_f \mathcal{C}_s$ , and (18) becomes a double integral evaluated with  $f_{\mathcal{C}}(\gamma_f \gamma_s) = f_{\mathcal{C}_f}(\gamma_f) f_{\mathcal{C}_s}(\gamma_s)$ .

### B. Nonadaptive Systems

Substituting (1) into (2), the information efficiency for non-adaptive systems is

$$IE = \sqrt{\frac{N}{\pi}} \tau(p) \epsilon [1 - F_{\mu}(\mu_c)] \quad (21)$$

where  $\mu_c$  is the appropriate cut-off SNR. In order to evaluate the information efficiency for various modulation schemes, we first need to determine the cut-off SNR values  $\mu_c$  assuming some coding scheme.

For the coding scheme, binary turbo-coded modulation is employed, where the information bits are encoded with a binary PCCC and mapped to a constellation symbol. At the receiver, prior to decoding, soft likelihood values are computed per

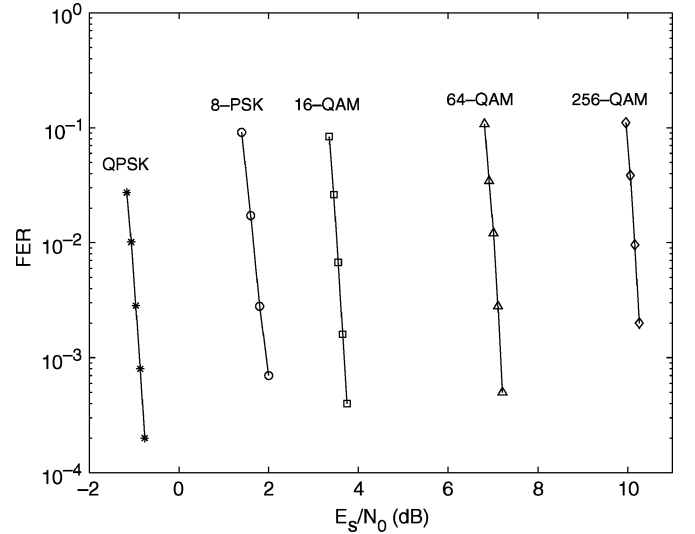


Fig. 3. FER versus SNR, rate-1/3 PCCC with  $(15, 13)_8$  RSC constituent encoder, 16 iterations, and 1500 channel symbols/frame.

TABLE I  
CUT-OFF SNRS,  $\mu_q$ , AND NORMALIZED CHANNEL GAIN THRESHOLDS,  
 $\gamma_{L,q}^*$  AND  $\gamma_{U,q}^*$ , BY MODULATION SCHEME

$q$	Modulation Scheme	$k_q$	$\mu_q$ (dB)	Capacity (dB)	$\gamma_{L,q}^*$	$\gamma_{U,q}^*$
1	QPSK	2	-1.1	-2.3	0	0.1422
2	8-PSK	3	1.7	0.1	0.1422	0.2095
3	16-QAM	4	3.5	1.9	0.2095	0.6058
4	64-QAM	6	7.0	5.0	0.6058	1.8729
5	256-QAM	8	10.2	7.7	1.8729	$\infty$

coded bit from the received channel symbols assuming knowledge of the SNR.<sup>4</sup> Encoding is based on a rate-1/3 PCCC with recursive systematic convolutional (RSC) constituent encoders having feedback and feed-forward generator polynomials of  $(15, 13)_8$ , respectively. The decoder utilizes the log-MAP algorithm for soft-input/soft-output iterative decoding.

Simulations were performed using this code in combination with the following coherent modulation schemes: QPSK, 8-PSK, 16-QAM, 64-QAM, and 256-QAM. The code interleaver size varied with the modulation scheme such that the frame size in channel symbols was constant at 1500 (i.e., a fixed slot duration). Since the fading attenuation is assumed to be fixed for the duration of a slot, and since the interference in a given slot is approximately Gaussian, the simulated channel was additive white Gaussian noise (AWGN). Results in terms of the frame error rate (FER) versus the symbol SNR after 16 decoding iterations are shown for each modulation scheme in Fig. 3. As can be observed, the performance of each modulation scheme with this code is characterized by a steep drop in FER around a certain SNR. For the purpose of obtaining specific results, the cut-off is defined here to be that SNR which yields an FER of  $10^{-2}$ . The cut-off SNRs, obtained from Fig. 3, are summarized in Table I by modulation scheme. Also included,

<sup>4</sup>While knowledge of the interference may be unavailable *a priori* for the purpose of adaptation as discussed later, it is reasonable to assume that it can be measured *after* the encoded frame is received for the purpose of MAP decoding.

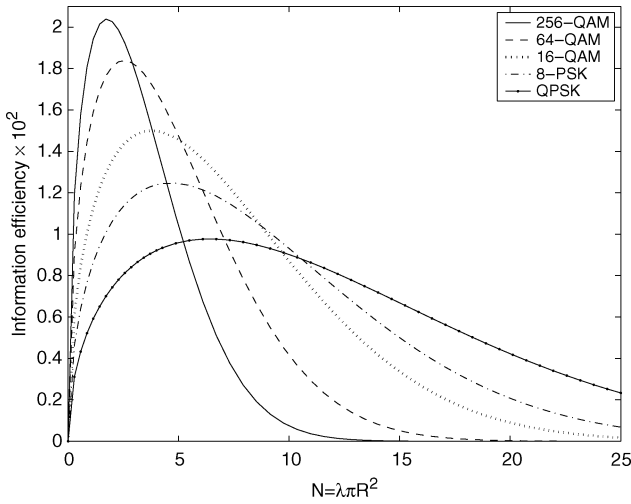


Fig. 4. Information efficiency versus  $N$  without fading or shadowing.

for comparison, are the capacity limits for these schemes, which are approximated from the mutual information for equiprobable inputs. We observe that this particular pragmatic encoder operates within 1.2–2.5 dB of capacity at an FER of  $10^{-2}$ , depending on the signal constellation used.<sup>5</sup>

Fig. 4 shows plots of information efficiency as a function of the normalized measure of link distance  $N$  for the various modulation schemes. These results are for channels with no fading or shadowing and were obtained using (21) and (19) with  $\gamma = 1$  and cut-off SNRs from Table I. In terms of system parameters, the spectral efficiency factor in (21) is  $\epsilon = kr/G$ , where  $k$  is the number of coded bits per constellation symbol and  $r$  is the code rate. For these and subsequent plots, an asynchronous CDMA system with rectangular chips and processing gain  $G = 11$  is assumed. The transmission probability  $p$  is 0.271, which was shown in [9] to optimize the expected progress, and, in this case, the information efficiency as well. We observe that each scheme is characterized by an optimum link distance at which information efficiency is maximized. As expected, 256-QAM performs best for short hop distances (for which the SIR is higher), while QPSK is best at longer distances, with the other modulation schemes being preferable at some intermediate ranges. The fact that higher order schemes can achieve greater information efficiency indicates that the increase in spectral efficiency on shorter links outweighs the resulting increase in the number of hops. However, the information efficiency with higher order schemes also experiences a more rapid decrease with increasing link distance due to their greater sensitivity to the SIR. Since link distance depends on the local topology and relay availability, robustness to a range of link distances can be preferable.

Fig. 5 shows the information efficiency as a function of  $N$  for several different channel scenarios. For these results, the modulation scheme is QPSK. The solid line in Fig. 5 is for the nonfading channel, and the other cases are for Ricean fading,

<sup>5</sup>In this analysis, we have chosen to keep the code rate fixed at  $1/3$  and only vary the modulation scheme. In general, the code rate could be varied as well to obtain other combinations of code rate and modulation scheme.

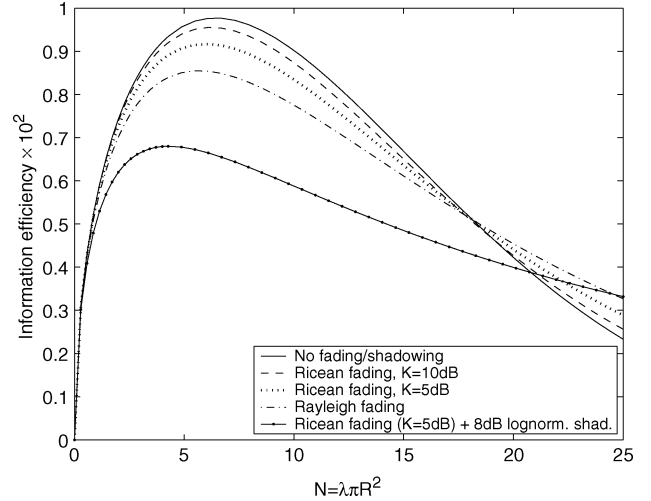


Fig. 5. Information efficiency with QPSK for various channel scenarios.

Rayleigh fading, and composite Ricean fading/lognormal shadowing. Except for extremely long transmission ranges, the impact of increasingly severe fading is to lower the information efficiency, as well as to reduce the transmission range at which it is maximized. The effect of a harsher channel is to: 1) render the desired link less reliable and 2) lessen the level of interference at the receiver. At most link distances, the former impact is predominant, while for very long distances the latter impact is more influential.

### C. Adaptive Systems

Adaptive modulation is considered here as a means of exploiting variable channel conditions to improve average performance given some knowledge of the channel state. Three types of adaptivity are examined, depending on the level of knowledge of the channel state that is available. In the first type, both the channel gain on the desired link and the level of interference at the receiver are known. However, in bursty packet radio networks, as modeled here, it is unlikely that *a priori* knowledge of the interference level for a future transmission would be available. Nevertheless, this type of adaptivity provides an upper bound on achievable performance with practical systems. The second type of adaptivity assumes knowledge of the channel gain only, which is typically correlated in time and can be measured and predicted [23]. The third type of adaptivity applies to situations in which the channel gain is made up of a fast fading component and a slowly varying component due to shadowing and distance, and only knowledge of the slowly varying component is available. Of interest is how these types of adaptivity perform relative to one another and to a nonadaptive scheme.

Using information efficiency as the metric to be optimized, an adaptive system selects the modulation scheme that maximizes the information efficiency given some knowledge of the channel state. Let  $\mathcal{S}$  represent the known channel state, and let  $Q$  be the number of modulation schemes available to the transmitter–receiver pair. Furthermore, let  $\epsilon_q$  be the spectral efficiency with modulation scheme  $q$ ,  $1 \leq q \leq Q$ , ordered such

that  $\epsilon_1 < \epsilon_2 < \dots < \epsilon_Q$ . Then, the information efficiency conditioned on channel state  $\mathcal{S}$  using modulation scheme  $q$  is

$$IE_q(\mathcal{S}) = \sqrt{\frac{N}{\pi}} \tau(p) \epsilon_q P_{s,q}(\mathcal{S}) \quad (22)$$

where  $P_{s,q}(\mathcal{S})$  is the conditional probability of successful transmission using modulation scheme  $q$ . The conditional information efficiency with adaptive modulation is the maximum of (22) over  $q$

$$IE_{AM}(\mathcal{S}) = \sqrt{\frac{N}{\pi}} \tau(p) \max_q \{ \epsilon_q P_{s,q}(\mathcal{S}) \}. \quad (23)$$

Averaging over channel states, the unconditioned information efficiency with adaptive modulation, in general, is

$$IE_{AM} = \sqrt{\frac{N}{\pi}} \tau(p) E_{\mathcal{S}} \left[ \max_q \{ \epsilon_q P_{s,q}(\mathcal{S}) \} \right].$$

1) *SIR Adaptivity*: In the case of SIR adaptivity, the known channel state  $\mathcal{S}$  is the SIR  $\mu$ . From (1), conditioned on the SIR, the conditional probability of success is simply

$$P_{s,q}(\mu) = u(\mu - \mu_q)$$

where  $\mu_q$  is the cut-off SIR for modulation scheme  $q$  and  $u(\cdot)$  is the unit step function. Following (23), the conditional information efficiency with SIR adaptivity is

$$IE_{AM,SIR}(\mu) = \sqrt{\frac{N}{\pi}} \tau(p) \max_q \{ \epsilon_q u(\mu - \mu_q) \}.$$

Averaging over the SIR, we have

$$\begin{aligned} IE_{AM,SIR} &= \sqrt{\frac{N}{\pi}} \tau(p) \int_0^{\infty} \max_q \{ \epsilon_q u(\mu' - \mu_q) \} f_{\mu}(\mu') d\mu' \\ &= \sqrt{\frac{N}{\pi}} \tau(p) \sum_{q=1}^Q \epsilon_q \int_{\mu_q}^{\mu_{q+1}} f_{\mu}(\mu') d\mu' \\ &= \sqrt{\frac{N}{\pi}} \tau(p) \sum_{q=1}^Q \epsilon_q [F_{\mu}(\mu_{q+1}) - F_{\mu}(\mu_q)] \end{aligned}$$

where  $\mu_{Q+1} \triangleq \infty$ .

2) *Signal Attenuation Adaptivity*: Though the statistics of the interference may be known, as noted earlier, the instantaneous interference in an upcoming slot may not be known. A more practical form of adaptivity may be one that adapts to the signal attenuation alone, in which case the known channel state  $\mathcal{S}$  is the attenuation factor  $\mathcal{C}$ . The conditional probability of success with modulation scheme  $q$ , conditioned on  $\mathcal{C} = \gamma$ , is

$$P_{s,q}(\gamma) = \Pr[\mu > \mu_q | \mathcal{C} = \gamma] = 1 - F_{\mu|C}(\mu_q | \gamma).$$

Hence, the conditional information efficiency with attenuation adaptivity is

$$IE_{AM,att}(\gamma) = \sqrt{\frac{N}{\pi}} \tau(p) \max_q \{ \epsilon_q [1 - F_{\mu|C}(\mu_q | \gamma)] \}. \quad (24)$$

Averaging over the channel attenuation, we have

$$IE_{AM,att} = \sqrt{\frac{N}{\pi}} \tau(p) \int_0^{\infty} \max_q \{ \epsilon_q [1 - F_{\mu|C}(\mu_q | \gamma)] \} f_C(\gamma) d\gamma. \quad (25)$$

Each modulation scheme maximizes the information efficiency for a given interval of the channel gain  $\gamma_{L,q} < \gamma < \gamma_{U,q}$ . The limits of these intervals or channel gain thresholds are such that

$$\epsilon_q F_{\mu|C}(\mu_q | \gamma) < \epsilon_{q'} F_{\mu|C}(\mu_{q'} | \gamma) \quad \forall q' \neq q, \gamma_{L,q} < \gamma < \gamma_{U,q}. \quad (26)$$

Furthermore, because the intervals are contiguous and span the entire range of  $0 < \gamma < \infty$ , the thresholds satisfy  $\gamma_{U,q} = \gamma_{L,q+1}$ ,  $\gamma_{L,1} = 0$ , and  $\gamma_{U,Q} = \infty$ . Rewriting (25) in terms of these thresholds, we obtain

$$IE_{AM,att} = \sqrt{\frac{N}{\pi}} \tau(p) \times \sum_{q=1}^Q \left\{ \int_{\gamma_{L,q}}^{\gamma_{U,q}} \epsilon_q [1 - F_{\mu|C}(\mu_q | \gamma)] f_C(\gamma) d\gamma \right\}. \quad (27)$$

The analysis above applies in general to channels with any path-loss exponent  $m > 2$  or fading statistics. For a path-loss exponent of  $m = 4$ , the conditional distribution of the SIR is given by (19). Specific values of the channel gain thresholds can be obtained by substituting this distribution in (26).<sup>6</sup> Table I lists these threshold values, normalized by  $(\beta N p)^2$ , for five coherent modulation schemes. Observation of the threshold values in Table I shows that the interval for which 8-PSK maximizes the information efficiency is relatively small, implying that, for the given coding system, not much additional gain is realized by including it in an adaptive scheme. This observation is also reflected in Fig. 4, which shows only a very small range for which 8-PSK performance exceeds that of the other schemes.

3) *Slow Adaptivity*: When the overall signal attenuation is due to a combination of small-scale fading, shadowing, and distance, in some cases, the system may be able to track and adapt to only the more slowly varying shadowing and distance-based components. The information efficiency with this form of slow adaptation is computed by replacing the conditional distribution in (27) with that averaged over the small-scale fading component and determining the thresholds (26) based on this new conditional distribution. For densities of the fading and shadowing

<sup>6</sup>In practice, the threshold values would incorporate the path loss due to distance, and a terminal would measure the overall attenuation  $\gamma/R^m$ . The attenuation due to distance is included in the parameter  $N$  here for ease of presentation.

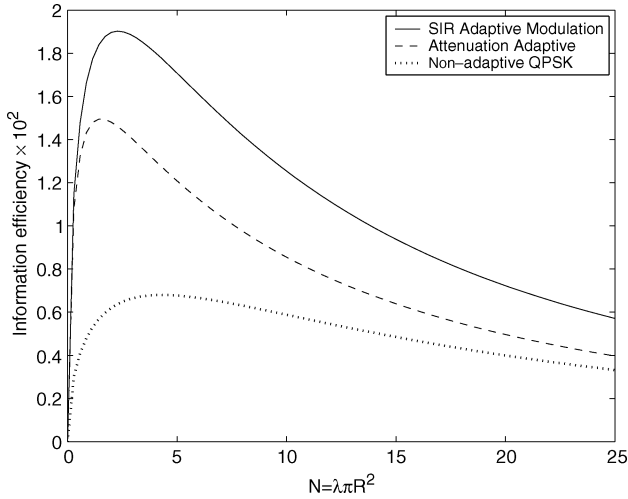


Fig. 6. Information efficiency versus  $N$  with Ricean fading ( $K = 5$  dB) and 8-dB lognormal shadowing: SIR adaptive, attenuation adaptive, and nonadaptive schemes.

attenuations of  $f_{C_f}(\gamma)$  and  $f_{C_s}(\gamma)$ , respectively, the information efficiency with slow adaptation is

$$\text{IE}_{\text{AM,slow}} = \sqrt{\frac{N}{\pi}} \tau(p) \sum_{q=1}^Q \int_{\gamma_{L,q}}^{\gamma_{U,q}} \epsilon_q f_{C_s}(\gamma_s) \times \left[ 1 - \int_0^{\infty} F_{\mu|C}(\mu_q | \gamma_f \gamma_s) f_{C_f}(\gamma_f) d\gamma_f \right] d\gamma_s.$$

4) *Quantitative Results:* Based on the preceding expressions, quantitative results are presented here for the information efficiency with the varieties of adaptive modulation defined above. As before, results are based on an assumption of asynchronous CDMA with rectangular chips, processing gain  $G = 11$ , and transmission probability  $p = 0.271$ . The channel gain is due to a combination of Ricean fading with Rice factor  $K = 5$  dB and 8-dB lognormal shadowing. Adaptive modulation is based on a set of four modulation schemes: QPSK, 16-QAM, 64-QAM, and 256-QAM.

Fig. 6 shows plots of information efficiency as a function of link distance in terms of  $N$ , comparing the performance of SIR adaptivity and attenuation adaptivity. The curve for nonadaptive QPSK is shown as well for reference. Each case is characterized by an optimum link distance at which information efficiency is maximized. The peak efficiency of the SIR adaptive and attenuation adaptive schemes is 2.8 and 2.2 times that of the nonadaptive scheme, respectively. Since a transmitter has only limited control over link distance in practice, a measure of overall performance is the information efficiency averaged over a distribution of link distances. Assuming a receiver position that is uniformly distributed in the transmission range  $0 < N < 25$ , SIR adaptivity still more than doubles the average information efficiency of nonadaptive QPSK, while attenuation adaptivity provides a 60% increase.

Fig. 7 illustrates results for two different kinds of attenuation adaptivity (i.e., for unknown interference), along with four nonadaptive schemes. The solid line marked with dots represents

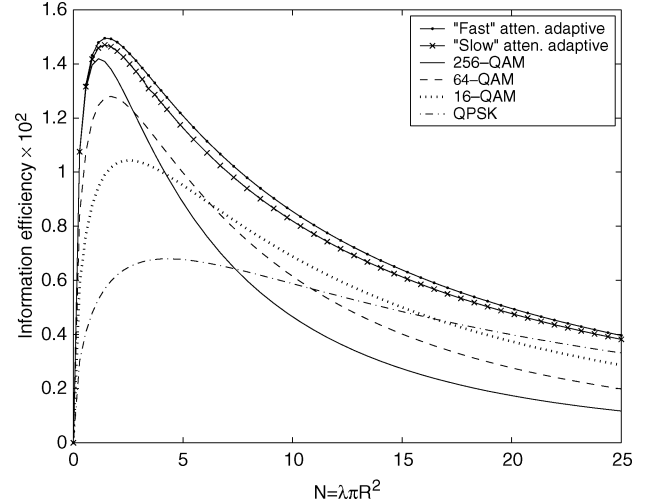


Fig. 7. Information efficiency versus  $N$  with Ricean fading ( $K = 5$  dB) and 8-dB lognormal shadowing: fast versus slow attenuation adaptive and nonadaptive schemes.

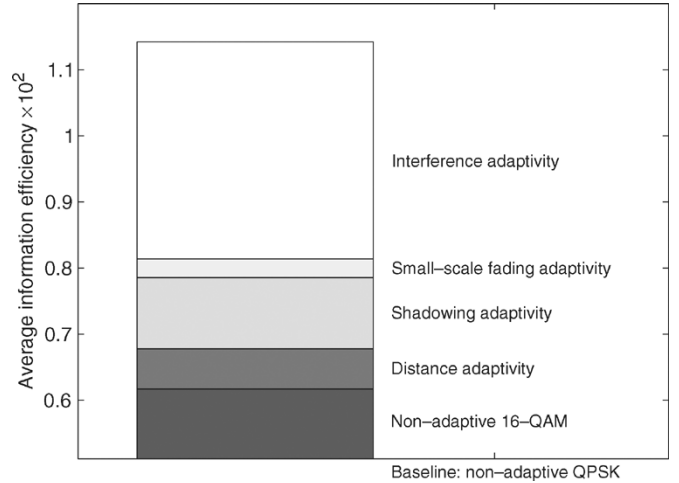


Fig. 8. Marginal benefits of adaptivity in Ricean fading ( $K = 5$  dB) and 8-dB lognormal shadowing.

“fast” attenuation adaptivity, based on knowledge of the combined shadowing and fading attenuation. The line marked with x’s represents “slow” attenuation adaptivity, based on knowledge of the shadowing (and distance-based attenuation) only. In both cases, the adaptive schemes exploit random variations in the channel due to fading and/or shadowing to selectively employ one modulation scheme over the others, resulting in a greater information efficiency than that achieved by any of the fixed modulation schemes alone. The adaptive schemes are also more robust to a range of link distances. While nonadaptive high-order modulation performs comparably at short range, and likewise low-order schemes at long range, the adaptive schemes perform better over the entire range.

Fig. 8 summarizes the relative benefits of the various forms of adaptivity in terms of their incremental gains in average information efficiency (averaged over  $0 < N < 25$ ). Slow adaptivity to distance and shadowing provides 85% of the benefit of full attenuation (fast) adaptivity over nonadaptive 16-QAM, indicating that adaptive modulation can be useful even in fast

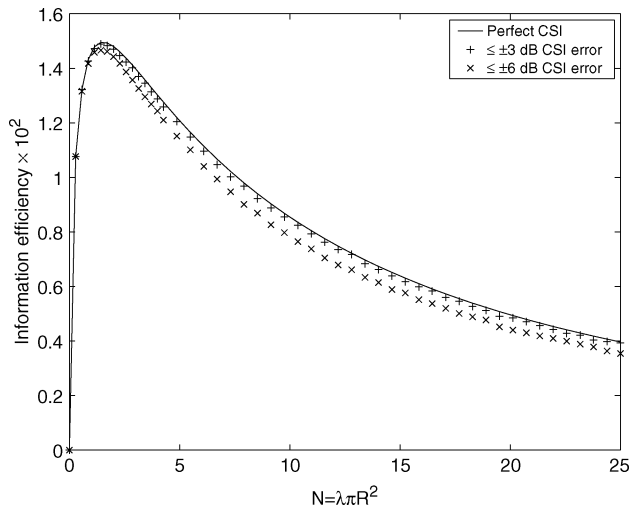


Fig. 9. Sensitivity of fast attenuation adaptivity to CSI error, in Ricean fading ( $K = 5$  dB) and 8-dB lognormal shadowing.

fading environments in which small-scale fading is difficult to track. When the fading is Rayleigh instead of Ricean, slow adaptivity provides 75% of the benefit of fast adaptivity.

Due to the limitations of practical channel estimators, as well as to the delay between the channel measurement and the adapted transmission, the adaptation in practice is based on imperfect channel information. To investigate the effect of imperfect channel information as well as imperfect knowledge of the channel gain thresholds, results assuming ideal information were compared with those obtained by introducing random errors into the channel gain estimates. The scope of this analysis is the effect on the adaptive choice of the modulation scheme and not on the decoding at the receiver, for which more timely, and therefore more accurate, measurements can be made. Fig. 9 compares the information efficiency with perfect channel information with that obtained by a Monte Carlo average of (24), where the modulation was selected using channel gain estimates uniformly distributed within  $\pm 3$  dB and within  $\pm 6$  dB, respectively, of the true fading/shadowing channel gains. The impact of these two levels of estimation error is a 1% and 7% reduction, respectively, in the average information efficiency. This robustness to imperfect side information can be expected, since only in channel states near the thresholds, or interval boundaries, are suboptimum decisions at risk of being made.

## V. CONCLUSION

A model for the performance analysis of multihop DS/CDMA networks of Poisson-distributed terminals was extended to account for a mixture of coherent modulation schemes, and an appropriate performance measure, information efficiency, was used to investigate the potential benefits of adaptive modulation in these networks.

By exploiting varying channel conditions on different links, adaptive modulation can be used in ad hoc networks to provide upper layers with higher capacity links over which to route traffic. Various forms of adaptivity were considered, including that based on knowledge of the current SIR, knowledge of the signal attenuation, and knowledge only of the slowly varying

components of the signal attenuation. While full knowledge of the SIR provides the best improvement, as it doubles the average information efficiency of a nonadaptive scheme, the difficulty of predicting the interference in bursty packet radio networks makes adapting to the signal attenuation a more practical approach. For channels with Ricean fading and lognormal shadowing, adapting to the combined fading/shadowing attenuation was found to increase the average information efficiency by 60%. The performance penalty of adapting to the shadowing component only, which is a form of slow adaptivity, is relatively small, indicating that most of the available gain can be realized with a more limited knowledge of the channel state. The analysis also indicates that the performance gain from adaptation is robust to imperfect channel information.

## REFERENCES

- [1] E. M. Royer and C.-K. Toh, "A review of current routing protocols for ad hoc wireless networks," *IEEE Pers. Commun.*, vol. 6, no. 2, pp. 46–55, Apr. 1999.
- [2] A. J. Goldsmith and S.-G. Chua, "Variable-rate variable-power MQAM for fading channels," *IEEE Trans. Commun.*, vol. 45, no. 10, pp. 1218–1230, Oct. 1997.
- [3] X. Qiu and K. Chawla, "On the performance of adaptive modulation in cellular systems," *IEEE Trans. Commun.*, vol. 47, no. 6, pp. 884–895, Jun. 1999.
- [4] S. Nanda, K. Balachandran, and S. Kumar, "Adaptation techniques in wireless packet data services," *IEEE Commun. Mag.*, vol. 38, no. 1, pp. 54–64, Jan. 2000.
- [5] E. S. Sousa and J. A. Silvester, "Optimum transmission ranges in a direct-sequence spread-spectrum multihop packet radio network," *IEEE J. Sel. Areas Commun.*, vol. 8, no. 5, pp. 762–771, Jun. 1990.
- [6] E. S. Sousa, "Performance of a spread spectrum packet radio network link in a Poisson field of interferers," *IEEE Trans. Inf. Theory*, vol. 38, no. 6, pp. 1743–1754, Nov. 1992.
- [7] J. Ilow, D. Hatzinakos, and A. N. Venetsanopoulos, "Performance of FH SS radio networks with interference modeled as a mixture of Gaussian and alpha-stable noise," *IEEE Trans. Commun.*, vol. 46, no. 4, pp. 509–520, Apr. 1998.
- [8] H. Takagi and L. Kleinrock, "Optimal transmission ranges for randomly distributed packet radio terminals," *IEEE Trans. Commun.*, vol. COM-32, no. 3, pp. 246–257, Mar. 1984.
- [9] M. Zorzi and S. Pupolin, "Optimum transmission ranges in multihop packet radio networks in the presence of fading," *IEEE Trans. Commun.*, vol. 43, no. 7, pp. 2201–2205, Jul. 1995.
- [10] M. W. Subbarao and B. L. Hughes, "Optimal transmission ranges and code rates for frequency-hop packet radio networks," *IEEE Trans. Commun.*, vol. 48, no. 4, pp. 670–678, Apr. 2000.
- [11] M. W. Chandra and B. L. Hughes, "Optimizing information efficiency in a direct-sequence mobile packet radio network," *IEEE Trans. Commun.*, vol. 51, no. 1, pp. 22–24, Jan. 2003.
- [12] *Higher Speed Physical Layer (PHY) Extension in the 2.4 GHz Band*, IEEE Std 802.11b/D8.0, Sep. 2001.
- [13] P. Gupta and P. R. Kumar, "The capacity of wireless networks," *IEEE Trans. Inf. Theory*, vol. 46, no. 2, pp. 388–404, Mar. 2000.
- [14] M. R. Souryal, B. R. Vojcic, and R. L. Pickholtz, "Interference model for ad hoc DS/CDMA packet radio networks with variable coherent modulation," in *Proc. MILCOM*, Oct. 2003, pp. 1–6.
- [15] G. Samorodnitsky and M. S. Taqqu, *Stable Non-Gaussian Random Processes: Stochastic Models With Infinite Variance*. New York, NY: Chapman & Hall, 1994.
- [16] R. K. Morrow, Jr. and J. S. Lehnert, "Bit-to-bit error dependence in slotted DS/SSMA packet systems with random signature sequences," *IEEE Trans. Commun.*, vol. 37, no. 10, pp. 1052–1061, Oct. 1989.
- [17] V. M. Zolotarev, *One-Dimensional Stable Distributions*. Providence, RI: American Mathematical Society, 1986.
- [18] W. Feller, *An Introduction to Probability Theory and Its Applications*, 2nd ed. New York, NY: Wiley, 1971, vol. 2.
- [19] T. Klingenbrunn and P. Mogensen, "Modeling cross-correlated shadowing in network simulations," in *Proc. Veh. Technol. Conf. (VTC)*, 1999, vol. 3, pp. 1011–1015.
- [20] T. S. Rappaport, *Wireless Communications: Principles & Practice*. Upper Saddle River, NJ: Prentice-Hall, 1996.

- [21] I. S. Gradshteyn and I. M. Ryzhik, *Table of Integrals, Series and Products*, 6th ed. New York, NY: Academic, 2000.
- [22] G. L. Stüber, *Principles of Mobile Communication*, 2nd ed. Boston, MA: Kluwer, 2001.
- [23] A. Duel-Hallen, S. Hu, and H. Hallen, "Long-range prediction of fading signals," *IEEE Signal Process. Mag.*, vol. 17, no. 3, pp. 62–75, May 2000.



**Michael R. Souryal** (M'89) received the B.S. degree in electrical engineering from Cornell University, Ithaca, NY, in 1990, the M.S. degree in information networking from Carnegie Mellon University, Pittsburgh, PA, in 1991, and the D.Sc. degree in electrical engineering from The George Washington University, Washington, DC, in 2003.

He is an NRC Postdoctoral Research Associate with the Wireless Communication Technologies Group, National Institute of Standards and Technology, Gaithersburg, MD. From 1991 to 1999, he was with Telcordia Technologies (formerly Bellcore), Red Bank, NJ, where he was involved in new service development for public network providers. His research interests include wireless ad hoc networks, cooperative diversity, spread-spectrum systems, and adaptive transmission techniques.



**Branimir R. Vojcic** (M'86–SM'96) received the Dipl.Ing., M.Sc., and D.Sc. degrees in electrical engineering from the University of Belgrade, Belgrade, Serbia and Montenegro, in 1980, 1986, and 1989, respectively.

Since 1991, he has been on the Faculty of The George Washington University, Washington, DC, where he is a Professor with, and former Chairman of, the Department of Electrical and Computer Engineering. His current research interests are in the areas of communication theory, performance evaluation and modeling of mobile and wireless networks, mobile internet, code-division

multiple access, multiuser detection, adaptive antenna arrays, space-time coding, and ad hoc networks. He has also been an industry consultant and has published and lectured extensively in these areas. He coauthored the book *The cdma2000 System for Mobile Communications* (Prentice-Hall, 2004).

Dr. Vojcic was a recipient of the National Science Foundation CAREER Award in 1995. He was an Associate Editor of the IEEE COMMUNICATIONS LETTERS and is presently an Associate Editor of the JOURNAL OF COMMUNICATIONS AND NETWORKS.



**Raymond L. Pickholtz** (S'54–A'55–M'60–SM'77–F'82–LF'96) received the Ph.D. degree in electrical engineering from the Polytechnic Institute, Brooklyn, NY.

He is a Professor Emeritus and former Chairman of the Department of Electrical and Computer Engineering, The George Washington University, Washington, DC. He was a Visiting Erskine Fellow with the University of Canterbury, Christchurch, NZ, in 1997. He has worked on many aspects of wireless communications including ad hoc networking, code-

division multiple-access satellite systems, digital audio broadcasting, and ultrawideband. He served on the FCC working group of the Spectrum Policy Task Force in 2002. He was named Co-Editor-in-Chief of the *Journal of Communications and Networks* in 2002 and now serves as its Editor-in-Chief.

Dr. Pickholtz is a Fellow of the American Association for the Advancement of Science. He was a recipient of the Donald W. McLellan Award in 1994 and the IEEE Millennium Medal in 2000. He coauthored the "Best Paper" of 1999 in the *Journal of Communications and Networks*. He has been an active member of the IEEE Communications Society, where he served as an Editor, Chairman of Major Conferences, the Board of Governors, and as President. He was the General Chairman of the IEEE INFOCOM, Kobe, Japan, in 1997 and of the ACM Mobicom, Boston, MA, in 2000.